Submitted to the American
Journal of Physics

LBL-1185
Preprint C.

INEXPENSIVE MECHANICAL MODEL OF A JOSEPHSON WEAK LINK

Gene I. Rochlin and Paul K. Hansma

October 1972

Prepared for the U.S. Atomic Energy
Commission under Contract W-7405-ENG-48

DISCLAIMER

LBL-1185
Preprint

Submitted to American Journal of Physics

UNIVERSITY OF CALIFORNIA

Lawrence Berkeley Laboratory
Berkeley, California

AEC Contract No. W-7405-eng-48

INEXPENSIVE MECHANICAL MODEL OF A JOSEPHSON WEAK LINK

Gene I. Rochlin and Paul K. Hansma

October 1972

Inexpensive Mechanical Model of a Josephson Weak Link

Gene I. Rochlin
Department of Physics, University of California
and
Inorganic Materials Research Division,
Lawrence Berkeley Laboratory,
Berkeley, California 94720

and

Paul K. Hansma
Department of Physics, University of California,
Santa Barbara, California 93106

ABSTRACT

We have built and used a simple, inexpensive mechanical model of a Josephson weak link consisting of a pendulum and an aluminum disk, both mounted on a common shaft. The pendulum is driven at constant torque by a weight hanging on a thread wrapped around the shaft and damped by the eddy currents induced in the aluminum disk by a permanent magnet. As this model has an equation of motion that is formally identical to the circuit equation proposed by Stewart and McCumber for a Josephson weak link, the differing I vs V characteristics of various weak links can be simulated and

understood with the model. The time evolution of the analogs of both the difference in phase across the weak link, ϕ , and the instantaneous supercurrent, $i_c \sin\phi$, can be directly observed. The low cost and reliability of the model makes it practical to construct in classroom quantities for undergraduate laboratories as a supplement to or substitute for conventional cryogenic Josephson effect experiments.

I. INTRODUCTION

The importance of the Josephson effect in superconductive tunneling both as a scientific problem and for device applications is beyond question. One of the most striking properties of Josephson junctions is that the quantum phase difference between the superconductors is observable, at least in principle. The introduction of this effect into the standard curriculum as an exposition of quantum phase effects has, however, been hampered by the fact that conventional experiments do not directly display the phase dependence which is implicit in the theory. The use of a mechanical analog, a driven, damped pendulum whose phase angle obeys the same equation of motion as the Josephson phase, lowers the period of phase rotation by a factor of 10^9 or greater, enabling the nonlinearity of the time dependence of the phase to be directly observed. The physical insight thus acquired is of inestimable value to student and teacher, as it has been to researchers in this field.

Sullivan and Zimmerman[1] have previously reported a mechanical analog which they constructed to illustrate Anderson's analogy[2] between the Josephson effect and a rotating pendulum in a gravitational field. Their model, while far more catholic than ours is also relatively complex and expensive, more suitable for lecture demonstrations or an advanced laboratory than for general use. We make no attempt to model the effects of external electromagnetic fields or the complex behavior of SQUIDS or other Josephson interference devices. Our model is most useful for visual observation of the time variation of the phase difference across a Josephson weak link as a function of its electrical

parameters. As such, a somewhat larger version might well be used for large lecture demonstrations. As a student laboratory experiment, measurements of the time-average rotational frequency vs the driving torque as a function of the pendulum mass, moment of inertia, and damping can be directly compared to the predictions of the theories of Stewart and McCumber[3] for the dc (average) voltage vs current characteristic of a Josephson weak link as a function of its resistance, capacitance, and critical supercurrent.

II. JOSEPHSON WEAK LINKS

Superconductivity was first observed by Kamerlingh Onnes in 1911 as an abrupt vanishing of the resistance of mercury below about 4.2K.[4] Following the subsequent discovery of perfect diamagnetism, the first macroscopic theories were developed by London and extended by Pippard.[5] The macroscopic theory reached its apex in the work of Ginzburg and Landau[5], who proposed that the onset of superconductivity is characterized by the appearance of a finite macroscopic "order parameter" ψ. This order parameter is position and field dependent, and much of their early work was devoted to solving for the dependence of ψ on currents and fields, and to its behavior near boundaries. As the order parameter is, in general, complex, it may be written as $\psi(r) = \sqrt{\rho(r)}e^{i\phi(r)}$, where $|\rho| = \psi^*\psi$ measures the strength of the ordering, and ϕ is the phase. This order parameter, although macroscopic, e.g., describing the entire piece of superconductor, resembles in many ways a wave function of ordinary quantum mechanics. In particular, as in time-independent solutions to the Schrödinger

equation, the position independent phase of an infinite superconductor in the absence of currents and fields is $\phi = \frac{Et}{\hbar} + \phi_o$, where E is the total energy of the superconducting charge carriers. For this reason, the order parameter is often called the superconducting wave function. It is important to emphasize, however, that this superconducting wave function describes the motion of all the superconducting conduction electrons--of the order of 10^{23} particles--rather than the few particles described by the usual quantum mechanical wave function.

In 1962, Josephson[6] studied the behavior of the order parameter in a system composed of two weakly coupled macroscopic pieces of superconductor. To define what Josephson meant by "weakly coupled", let us consider the limits first of no coupling and then of very strong coupling. If the two pieces are not coupled at all, the phase of the order parameter of one will be completely independent of the phase of the order parameter of the other; the phase of either can be changed by an arbitrary phase factor without affecting any external physical observables. In the opposite limit, in which the two pieces are joined together to form one larger piece, there can be no abrupt change in the phase of the order parameter across the boundary because of the long range order of the phase due to the motion of conduction electrons from one piece to the other.[6,7] The interesting case discussed by Josephson is that of weak coupling, in which the phases are still correlated (i.e., the phase of one cannot be changed by an arbitrary phase factor without affecting the phase of the other) but a phase difference can exist between the pieces. This weak coupling can be obtained in many different ways; by simply placing the two pieces in

close physical proximity (≈ 20 Å separation) for example.

Josephson first derived the dependence of the difference in the phase, ϕ, of the order parameter between two superconductors on the supercurrent, i_s, and voltage, V, between them. The predictions are called the dc and ac Josephson equations respectively:

$$\phi = \arcsin(i_s/i_c) \tag{1a}$$

$$\frac{d\phi}{dt} = \frac{2e}{\hbar} V, \tag{1b}$$

where he has assumed that the charge carriers are superconducting pairs,[5,6] and therefore that the energy difference per pair across a voltage V is simply $\delta E = 2eV$. Here i_c, called the critical current, is the maximum current for which there is a zero-voltage supercurrent solution to the equations (i.e., $\phi = \arcsin(i_s/i_c), d\phi/dt = 0$). The magnitude of this critical current depends on the strength of the coupling. For example, if the weak coupling is obtained through physical proximity by placing the pieces a distance d apart, the critical current, i_c, varies as:

$$i_c \propto \exp(-d/d_o) \tag{2}$$

where d_o is on the order of 1Å.

Since this theoretical treatment, many actual devices have been constructed. These devices are collectively known as "weak links" since their common feature is that they weakly couple or weakly link

two pieces of superconductor. A selection of these devices is shown in Fig. 1. Figure 1a shows a superconducting metal-insulator-superconducting metal (S-I-S) thin film tunneling junction.[8] This type of junction is formed by first evaporating one metal strip, then oxidizing it according to some recipe (e.g., heating to 100°C in pure oxygen for 3 hours), and finally evaporating a cross strip to complete the junction. The necessary weak coupling is obtained by the close physical proximity of the two superconducting metal films; where they cross they are separated by an oxide layer on the order of 20 Å thick. Figure 1b shows a superconducting metal-normal metal-superconducting metal (S-N-S) thin film junction[9] in which the insulating layer separating the two superconducting metal films in the S-I-S junction is replaced by a much thicker layer of normal metal. A very different device is the point contact[10,11] shown in Fig. 1c. Here the weak coupling is due to the small area of contact between a sharpened superconducting rod and a superconducting block against which the rod is lightly pressed. Other devices exhibit still other experimental methods of obtaining the necessary weak coupling, but are all based on one of these three principal methods.

All of these weak links will carry supercurrents up to a certain maximum supercurrent, i_c, as predicted by Josephson; if the current through such a device is slowly increased from zero by means of an external current supply, no voltage will develop across it until the critical current is exceeded. (An external voltage supply is generally of less interest since the impedance of these devices is usually very small.) Above the critical current a non-zero voltage always develops

but, nevertheless, the nonzero current-voltage (I-V) characteristics of these devices differ widely. For example, in the S-N-S junction[9] the voltage develops smoothly from zero when the critical current is exceeded; as the current is decreased again the voltage decreases along the same curve: there is no hysteresis in the I-V characteristic. On the other hand, for some other devices,[3,12] the voltage develops abruptly when the critical current is exceeded; the voltage jumps discontinuously from zero to some finite value in a time on the order of 10^{-10} sec. and as the current is further increased, the voltage increases smoothly. When the current is decreased, the voltage decreases smoothly along the same curve until the critical current is reached. At this point the voltage does not drop discontinuously to zero again. Rather, as the current is further decreased the voltage continues to decrease smoothly, not going to zero until the current is well below the critical current. Consequently for some values of current there are two solutions for the voltage, a zero voltage supercurrent solution and a nonzero voltage solution; there is hysteresis in the I-V characteristic. For the S-I-S junction[8] the hysteresis is almost complete. As the current is decreased from above the critical current the voltage does not decrease to zero until the current is almost zero. Thus, for the S-I-S junction there are two solutions for the voltage for almost all currents between zero and the critical current.

In an effort to unify the theoretical treatment of these diverse devices, Stewart and McCumber independently developed a theory[3] to explain why the I-V characteristics of one type of weak link differed so markedly from that of another. In particular, their theory showed

that the differences in I-V characteristics could be explained by taking into account the different ac and dc impedances of the various devices. Previously, there had been speculation that the substantial qualitative differences in the I-V characteristics (most strikingly the difference in the amount of hysteresis) were a result of quite different mechanisms for supercurrent flow; i.e., there was speculation that the work of Josephson did not apply to all these devices without some modification.

The Stewart-McCumber theory, however, showed that at least the main qualitative differences (including the wildly varying hysteresis) could be explained by a lumped circuit model that included the distributed internal resistance and capacitance of the devices in parallel with an idealized Josephson junction described by the Josephson equations. This idealized junction passes only supercurrent and dissipates no energy since

$$\langle i_s V \rangle_t = \lim_{T\to\infty} \frac{1}{T} \int_{To}^{T} \frac{2ei_c}{\hbar} \sin\phi \frac{d\phi}{dt}\, dt$$

$$= \frac{2ei_c}{\hbar} \lim_{T\to\infty} \frac{1}{T} \int_{\phi_o}^{\phi(T)} d(\cos\phi) \leq \frac{4ei_c}{\hbar} \lim_{T\to\infty} \left(\frac{1}{T}\right) = 0.$$

This lumped circuit model is shown in Fig. 2. The total current, I, is the sum of three terms: (1) the current through the capacitor, C(dV/dt), where C is the capacitance and V is the voltage across the circuit; (2) the current through the resistor, GV, where G is its conductance; and (3) the Josephson supercurrent, $i_c \sin\phi$, where i_c is the critical current and ϕ is the difference in the phase of the

superconducting wave function across the junction. That is:

$$I = C\frac{dV}{dt} + GV + i_c \sin\phi. \tag{3}$$

In writing this equation we have used only elementary circuit theory and the dc Josephson equation (Eq. 1a). By using the ac Josephson equation (Eq. 1b) we can eliminate the voltage, thus obtaining the equation

$$I = \frac{C\hbar}{2e}\frac{d^2\phi}{dt^2} + \frac{G\hbar}{2e}\frac{d\phi}{dt} + i_c \sin\phi. \tag{4}$$

This equation can be reduced to dimensionless form by dividing through by the critical current and substituting a dimensionless time $\tau = (2e/\hbar)(i_c/G)t$. The resulting equation is

$$\frac{I}{i_c} = \beta_c \frac{d^2\phi}{d\tau^2} + \frac{d\phi}{d\tau} + \sin\phi, \tag{5a}$$

where

$$\beta_c \equiv \frac{2e}{\hbar} i_c \frac{C}{G^2} \tag{5b}$$

is a dimensionless circuit parameter that determines the shape of the I vs $\langle V \rangle$ curve and the amount of hysteresis.

This equation can be solved for the time-averaged voltage,

$$\langle V \rangle_t = \left(\frac{\hbar}{2e}\right) \left\langle \frac{d\phi}{dt} \right\rangle_t = \left(\frac{i_c}{G}\right) \left\langle \frac{d\phi}{d\tau} \right\rangle_\tau, \tag{6}$$

as a function of the current, I. Computer generated solutions for

various values of β_c are shown in Fig. 3. The main difference between the solutions for different values of β_c is in the amount of hysteresis in the I-V characteristic, that is, the range of current over which there is both a zero bias and a finite bias solution. Following McCumber, we can define a hysteresis parameter, α, as the ratio of the minimum current as the voltage goes to zero to the critical supercurrent. This α ranges from 1 in the case of no hysteresis (low β_c) to 0 in the case of maximum hysteresis (high β_c). Figure 4 shows McCumber's results from solving Eq. (5) for α as a function of β_c.

These theoretical results can be compared to experimental results[12] we have obtained with a particularly versatile weak link, the externally shunted oxide barrier junction. For this type of weak link the conductance G, is not merely the inherent quasiparticle conductance of the junction, but rather the parallel combination of this quasiparticle conductance with the usually much larger shunt conductance. By varying the shunt conductance or the critical current, β_c can be varied over a wide range. Figures 5 and 6 show our experimental results for I vs V and α vs β_c respectively. Note that all the results in each figure were obtained with a single shunted junction.

III. MECHANICAL MODEL

A. Theory

Consider the driven, damped simple pendulum shown in Fig. 7. The fundamental equation for the angular displacement is $T = M\,(d^2\theta/dt^2)$, torque equals moment of inertia times angular acceleration. The total

torque has three components: (1) the applied torque, $T_a = m_w gr$, where m_w is the mass of the hanging weight, g is the acceleration due to gravity, and r is the radius of the shaft; (2) the opposing torque from the pendulum bob, $-T_c \sin\theta = -mg\ell \sin\theta$, where m is the mass of the pendulum bob and ℓ is the length of the pendulum; (3) the opposing torque from the damping, $-D(d\theta/dt)$, where D is the damping coefficient. Thus the fundamental equation is:

$$T_a - T_c \sin\theta - D\frac{d\theta}{dt} = M \frac{d^2\theta}{dt^2} . \tag{7}$$

By rearranging terms we obtain:

$$T_a = M \frac{d^2\theta}{dt^2} + D \frac{d\theta}{dt} + T_c \sin\theta . \tag{8}$$

Note the exact analogy between the equation for the electrical model, Eq. (4), and this equation for the mechanical model. The mechanical analogies to the electrical parameters are listed in Table I. For the Josephson weak link we are most interested in the time-averaged voltage, $\langle V \rangle_t = (\hbar/2e) \langle d\phi/dt \rangle_t$, as a function of applied current. By analogy, for the mechanical model we are most interested in the time-averaged rate of rotation, $\langle d\theta/dt \rangle_t$ as a function of applied torque. The other elements of the analogy can be easily understood. For example, the capacitance is analogous to the moment of inertia: in the electrical case the capacitance tends to keep the voltage constant while in the mechanical case the moment of inertia tends to keep the angular velocity constant. The conductance is analogous to the damping

coefficient: in the electrical case the conductance passes a current proportional to voltage, while in the mechanical case the damping coefficient causes a torque proportional to angular velocity.

B. Description

The mechanical model is shown in Fig. 8a,b. It consists of a pipe cleaner pendulum driven at constant torque by brass washers hanging on thread wrapped around the pendulum axle. The pendulum bob is cut from a playing card and glued to the pipe cleaner. The motion is damped by eddy currents induced in the aluminum disk by the permanent magnet. The only critical part of the construction is the shaft bearing. This is because the total torque is at times very small; for example, when the pendulum bob is only a few degress from arcsin (T_a/T_c), the total torque is on the order of 100 dyne-cm (10^{-3} oz-in). Although not much friction can be tolerated, inexpensive (nonmagnetic!) unshielded ball bearings work well if used in pairs. The aluminum bearing post of the model shown in Fig. 8 contains one bearing press-fit into each side.

C. Operation

After preliminary experimentation to gain familiarity with the model, systematic experimentation can begin. First the damping is fixed at some value by taping the magnet to the base (double-stick masking tape is ideal). Then a plot like those of Fig. 9 is obtained by measuring the equilibrium rate of rotation as a function of applied torque (i.e., number of washers hanging). A convenient way to measure the rate of rotation is to time ten or twenty periods with a stop watch.

It is, of course, important not to include the first few periods, but rather wait until an equilibrium rate of rotation is achieved.

Two simple experiments determine "β_c". The ratio D/T_c is determined by first adjusting the hanging weight until $T_a = T_c$ by adding weight until the pendulum bob will remain stationary at $\theta \cong 90°$. Then the pendulum bob is removed and the equilibrium rate of rotation from this torque is measured with a stop watch. If the measured time for one complete rotation is t_1, then we have $T_c = D\,\frac{2\pi}{t_1}$. Hence the desired ratio D/T_c, is equal to $\frac{t_1}{2\pi}$. Next the ratio $\frac{M}{T_c}$ can be determined by measuring the period of small oscillations around $\theta = 90°$ with no applied torque and no damping. For small oscillations the equation of motion is $M\ddot{\theta} = -T_c\,\theta$, with a period $t_2 = 2\pi\,\frac{M}{T_c}$. Thus the desired ratio $\frac{M}{T_c}$, is equal to $\left(\frac{t_2}{2\pi}\right)^2$. Multiplying the square of the first ratio times the second, we obtain

$$"\beta_c" \equiv \frac{T_c M}{D^2} = \left(\frac{t_2}{t_1}\right)^2. \tag{9}$$

After plotting the rate of rotation vs applied torque curve and determining corresponding"β_c", the damping is changed by moving the magnet and the new curve plotted. Note that to determine"β_c" for this second curve only t_1 must be measured since t_2 is unchanged. Alternately, the magnet can be left fixed and the length of the pendulum changed by sliding the pipe cleaner through the shaft. In this case, however, both t_1 and t_2 must be remeasured.

Intuition is quickly developed during a few such plots.[13] One of the most important points is why"β_c" determines the amount of hysteresis

in the plot. Though this is difficult to understand for a Josephson weak link, the mechanical model makes it clear. For any $T_a < T_c$ there is an unstable region from $\theta = \theta_c$ ($\equiv \arcsin\left(\frac{T_a}{T_c}\right)$) to $\theta = (180° - \theta_c)$ in which the total torque is negative. If the pendulum bob ever stops in this region it will fall back and come to rest in the nonrotating solution, $\theta = \theta_c$. There will be a rotating solution only if the moment of inertia is large enough relative to the damping so that the kinetic energy of the pendulum can carry it through the unstable region. A normalized measure of the moment of inertia is t_2^2; the corresponding normalized measure of damping is t_1^2. It is their ratio, "β_c" $\equiv \left(\frac{t_2}{t_1}\right)^2$, that determines whether or not there will be a rotating solution at this value of applied torque. That is, it is "β_c" that determines the amount of hysteresis in the plot of rate of rotation vs applied torque.

The advantages of viewing the model rather than reading a written description become overwhelming in studying the nonlinearities of the time evolution of the phase. Consequently we will not even attempt a written description here. Important points to note when viewing the model are: (1) Under what conditions is the time averaged torque from the pendulum bob nonzero? (i.e., under what conditions is the time averaged supercurrent nonzero?) (2) Under what conditions does the rate of rotation become very nonlinear? (i.e., under what conditions are there large voltage variations with time?) (3) Why do these nonlinearities occur?

A feature of the model that invites further experiments is that the length of pendulum when viewed from above, $\ell \sin\theta$, has the same

dependence on angle as the supercurrent in a Josephson weak link, $I_c \sin\phi$, has on phase. Thus, viewing the pendulum from above during its motion shows the time dependence of the supercurrent in a Josephson weak link under analogous conditions ($I/I_c = T_a/T_c$, "β_c" = β_c). Frame by frame examination of a motion picture taken from above would be especially instructive; a graph of the time dependence could be made.

D. Experimental Results

Figure 9 shows experimental results for the rate of rotation vs applied torque for various values of "β_c". The length of the pendulum and mass of the pendulum bob were adjusted until the critical torque T_c corresponded to ten 4.6 gm brass washers (ordinary 5/16" washers). The mass of the pendulum bob was adjusted by adding tape until T_c was almost correct; fine adjustments were made by sliding the pipe cleaner into or out of the shaft. Then, for the four runs shown, the damping was adjusted until the pendulum just barely ran with 10, 9, 6, and 2 washers respectively.

After a complete rate of rotation vs applied torque curve was plotted, t_1 was determined by measuring the rate of rotation with no pendulum at the maximum torque used for the curve. (These points are not shown in the curves of Fig. 9.) The dashed line from these points through the origin represents the rate of rotation vs torque as determined purely by damping. The parameter t_1 is obtained by reading the period for $T_a = T_c$ from the dashed line; $t_1 = 1/f_o$ in the units of Fig. 9.

After all of the curves were completed, t_2 was determined by measuring the period of small oscillations with $T_a = 0$ and no damping. Using Eq. (9) the values of "β_c" were then computed for all of the

curves. The values of α were obtained by extrapolating the curves to zero rate of rotation. The α vs "β_c" values for the curves of Fig. 9 are plotted in Fig. 10. The solid line is the computer generated result from a theoretical paper[3] on Josephson weak links. It should be emphasized that there are no adjustable parameters in plotting the results.

The excellent agreement between the experimental results obtained with the model and the computer generated theoretical results confirms the adequacy of our theoretical treatment: the corrections for air resistance, bearing friction, non-uniformity of applied torque, etc. are clearly negligible. Thus, the model not only gives good qualitative understanding of a Josephson weak link, it also gives correct quantitative results. It could, for example, be used to predict the performance of a weak link with arbitrary C, G, and i_c. If the undergraduate laboratory is equipped with cryogenic apparatus, this mechanical model can be used in conjunction with an externally shunted Josephson junction[12] to provide a complete explication of the dc Josephson effect in weak link geometries. The externally shunted junction can be fitted to theory using only C as a fitting parameter. The validity of this procedure is readily shown with the mechanical model.

IV. SUMMARY

An inexpensive mechanical model shown in Fig. 8 is a valuable tool for learning about Josephson weak links. It can be used to obtain quantitative predictions for the Γ vs V characteristics of weak links with arbitrary internal capacitance, conductance, and critical current. Even more important, it gives a detailed insight into the reasons for the behavior of weak links. The time evolution of both the difference in phase of the order parameter across the weak link, ϕ, and the instantaneous supercurrent through it, $i_c \sin\phi$, can be observed directly. Both as a problem in non-linear mechanics and as an illuminator of observable quantum phase effects, the model is an ideal teaching device.

V. ACKNOWLEDGEMENTS

We wish to thank Ted Fulton, John Clarke, Paul Richards, and Don Whitaker for valuable discussions and suggestions.

This work was performed under the auspices of the U. S. Atomic Energy Commission.

REFERENCES

1. D. B. Sullivan and J. E. Zimmerman, Am. J. Phys. 39, 1504 (1971).

2. P. W. Anderson, Lectures on the Many-Body Problem, E. R. Caianello, Ed. (Academic Press, N.Y., 1964), Vol. 2.

3. W. C. Stewart, Appl. Phys. Letters 12, 277 (1968); D. E. McCumber, J. Appl. Phys. 39, 3113 (1968).

4. H. Kamerlingh Onnes, Akad. van Wetenschappen (Amsterdam) 14, 113, 818 (1911).

5. See, for example, the review articles by N. R. Werthamer and by B. S. Chandrasekhar, in Superconductivity, R. D. Parks, Ed. (Marcel Dekker, Inc., New York, 1969), Vol. I.

6. B. D. Josephson, Phys. Letters 1, 251 (1962); Rev. Mod. Phys. 36, 216 (1964); Advan. Phys. 14, 419 (1965).

7. See also the review article by J. E. Mercereau, in Superconductivity (ibid.).

8. P. W. Anderson and J. M. Rowell, Phys. Rev. Letters 10, 230 (1963).

9. J. Clarke, Proc. Roy. Soc. A308, 447 (1969).

10. J. E. Zimmerman and A. H. Silver, Phys. Rev. 141, 367 (1966).

11. L. J. Barnes, Phys. Rev. 184, 434 (1969).

12. P. K. Hansma and G. I. Rochlin, to be published in J. Appl. Phys. October 1972; P. K. Hansma, G. I. Rochlin and J. N. Sweet, Phys. Rev. B4, 3003 (1971).

13. This position was succinctly stated by Lord Kelvin in his Baltimore Lectures (Baltimore: Publication Agency of Johns Hopkins University, 1904); "I never satisfy myself until I can make a mechanical model of a thing. If I can make a mechanical model, I can understand it. As long as I cannot make a mechanical model all the way through

I cannot understand: and that is why I cannot get the electromagnetic theory...": as quoted by S. L. Jaki in The Relevance of Physics (University of Chicago Press, Chicago, 1966), p. 75.

TABLE I

MECHANICAL ANALOGS TO ELECTRICAL PARAMETERS

Electrical System	Mechanical System
$\phi \equiv$ difference in phase of superconducting wave function across Josephson junction	$\theta \equiv$ angle measured in direction of applied torque from vertically downward to pendulum bob
$\frac{d\phi}{dt} = (\frac{2e}{\hbar})V$ = voltage $\times$ $(\frac{2e}{\hbar})$	$\frac{d\theta}{dt}$, the angular frequency
$i_c \equiv$ maximum Josephson supercurrent	$mg\ell \equiv$ maximum torque from pendulum bob
$I \equiv$ externally supplied current	$T_a \equiv$ externally supplied torque from eddy current drive
$(\frac{\hbar}{2e})$ C capacitance $\times$ $(\frac{\hbar}{2e})$	M where M is the moment of inertia of the disk plus pendulum bob
$(\frac{\hbar}{2e})$ G conductance $\times$ $(\frac{\hbar}{2e})$	D where D is the damping coefficient of the eddy current damping (damping torque = $D \frac{d\theta}{dt}$)

FIGURE CAPTIONS

Fig. 1. An assortment of weak-link Josephson effect devices: (a) superconductor-insulator-superconductor (S-I-S) thin film tunnel junction; (b) superconductor-normal metal-superconductor (SNS) thin film junction; (c) point contact junction.

Fig. 2. The equivalent circuit for a non-inductive weak link driven by a constant current source. As C is an ideal capacitor and the Josephson element only passes ac and dc supercurrent, the power dissipated in this circuit must all be dissipated in the shunt conductance G.

Fig. 3. Theoretical results (Ref. 3) for the time-averaged voltage vs current as a function of β_c for a device having the equivalent circuit shown in Fig. 2. These curves are after McCumber; Stewart's similar results are labeled with the parameter $\omega_o\tau = (\beta_c)^{1/2}$.

Fig. 4. McCumber's universal plot of the hysteresis parameter $\alpha \equiv (i_{min}/i_c)$ as a function of the dimensionless circuit parameter β_c.

Fig. 5. Experimental results for time-averaged voltage vs current for an externally shunted Josephson junction (Ref. 12) as a function of β_c. These results should be compared with the theoretical results shown in Fig. 3.

Fig. 6. β_c vs α plot for an externally shunted Josephson junction similar to that shown in Fig. 5. To vary β_c, a small magnetic field was applied parallel to the plane of the junction; this decreased i_c without altering C or G. The solid line is the

theoretical curve of Fig. 4. The only adjustable parameter was the capacitance of the junction.

Fig. 7. Schematic diagram of the pendulum of the mechanical model, driven by a weight attached to a string wrapped about the shaft. The applied torque is $T_a = m_w g r$; the pendulum torque is $T = -T_c \sin\theta = -mg\ell \sin\theta$. The damping disk is not shown.

Fig. 8. Two views of the small mechanical model.

(a) Frontal view, showing the pendulum, the aluminum damping disk, and one of the bearings supporting the shaft.

(b) Side view, showing the small horseshoe magnet which provides the damping field, the drive string wrapped around the shaft, and the aluminum frame. The bearing support arm is fastened to the base plate with screws, and the base plate is cut away beneath the disk so that the magnet is not too close to the rim. All fittings and parts are nonmagnetic, and it is best not to wear the timing watch!

Fig. 9. Experimental results for time-averaged rotation rate (f) vs applied torque (number of washers hung on the hook) for the mechanical model shown in Fig. 8. The critical torque corresponds to ten washers; rotating solutions for less than ten are obtained by flipping the pendulum to get it started. The method of obtaining the data and the derivation of β_c are described in the text.

Fig. 10. The experimental results of Fig. 9 plotted as β_c vs α. The solid line is the theoretical curve of McCumber as calculated for the mechanical model, with no adjustable parameters.

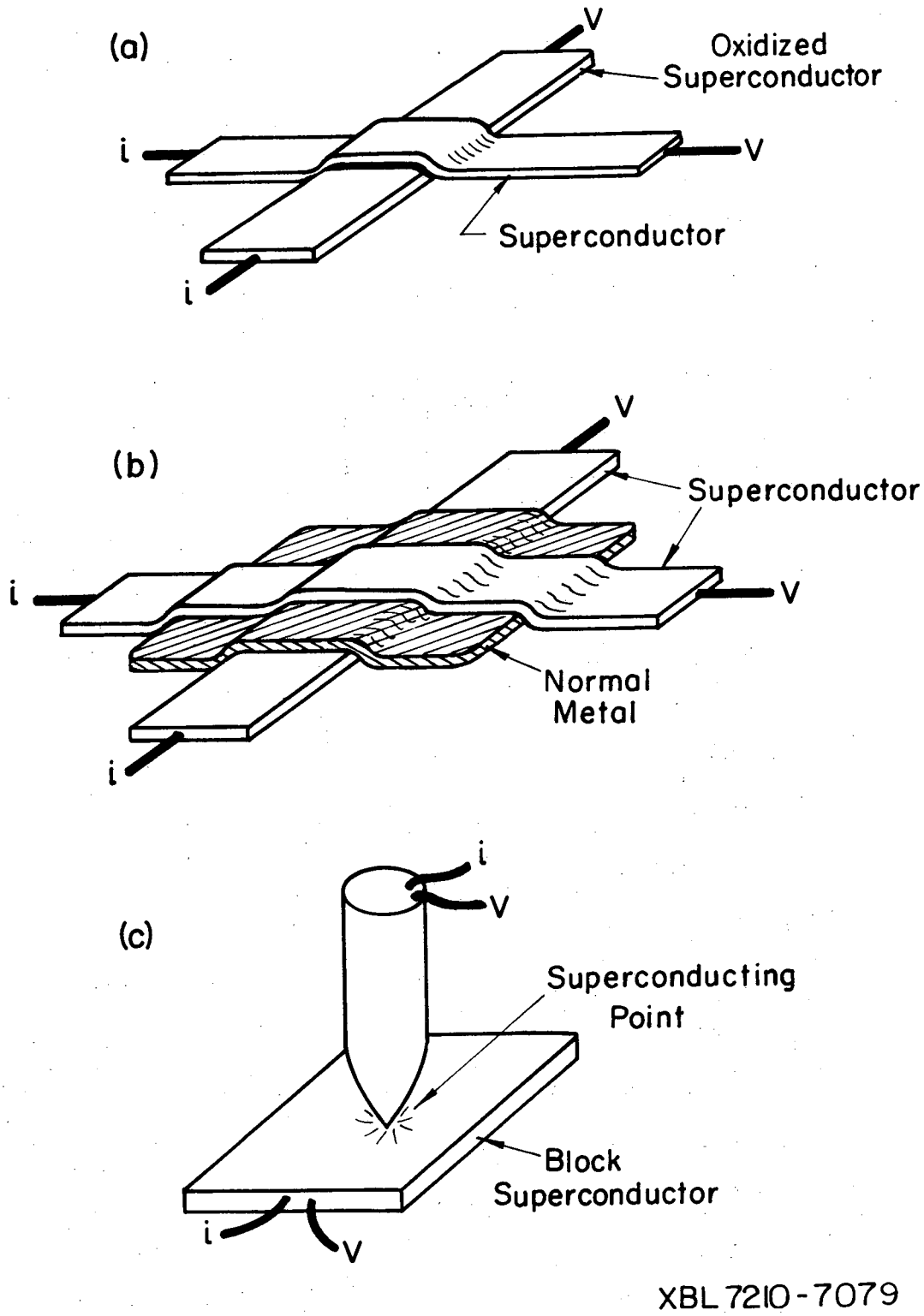
(a)
V
Oxidized
Superconductor
i
V
Superconductor
i
(b)
V
Superconductor
i
V
Normal
Metal
i
(c)
i
V
Superconducting
Point
Block
Superconductor
i
V
XBL 7210-7079

Fig. 1

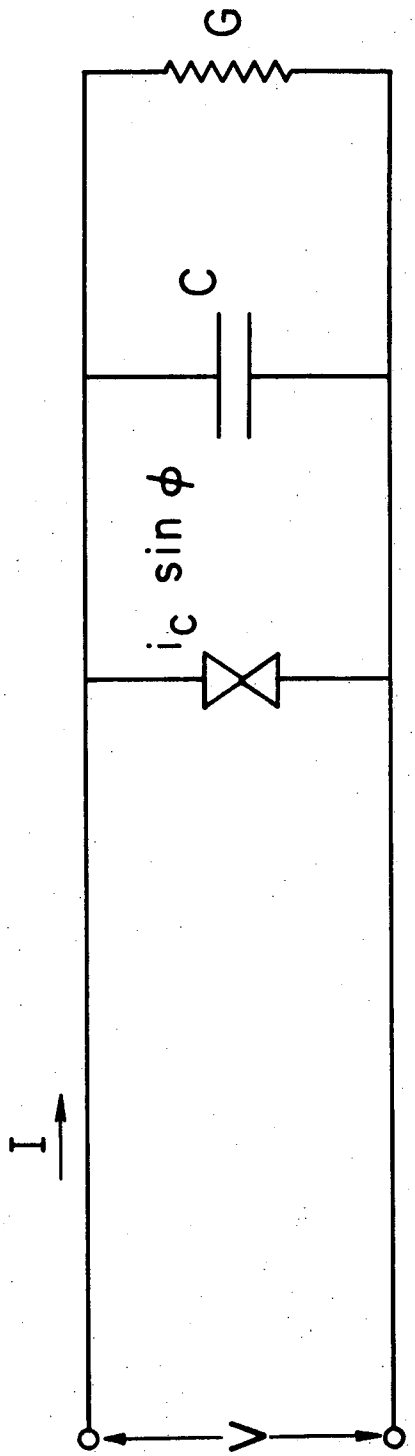

Fig. 2

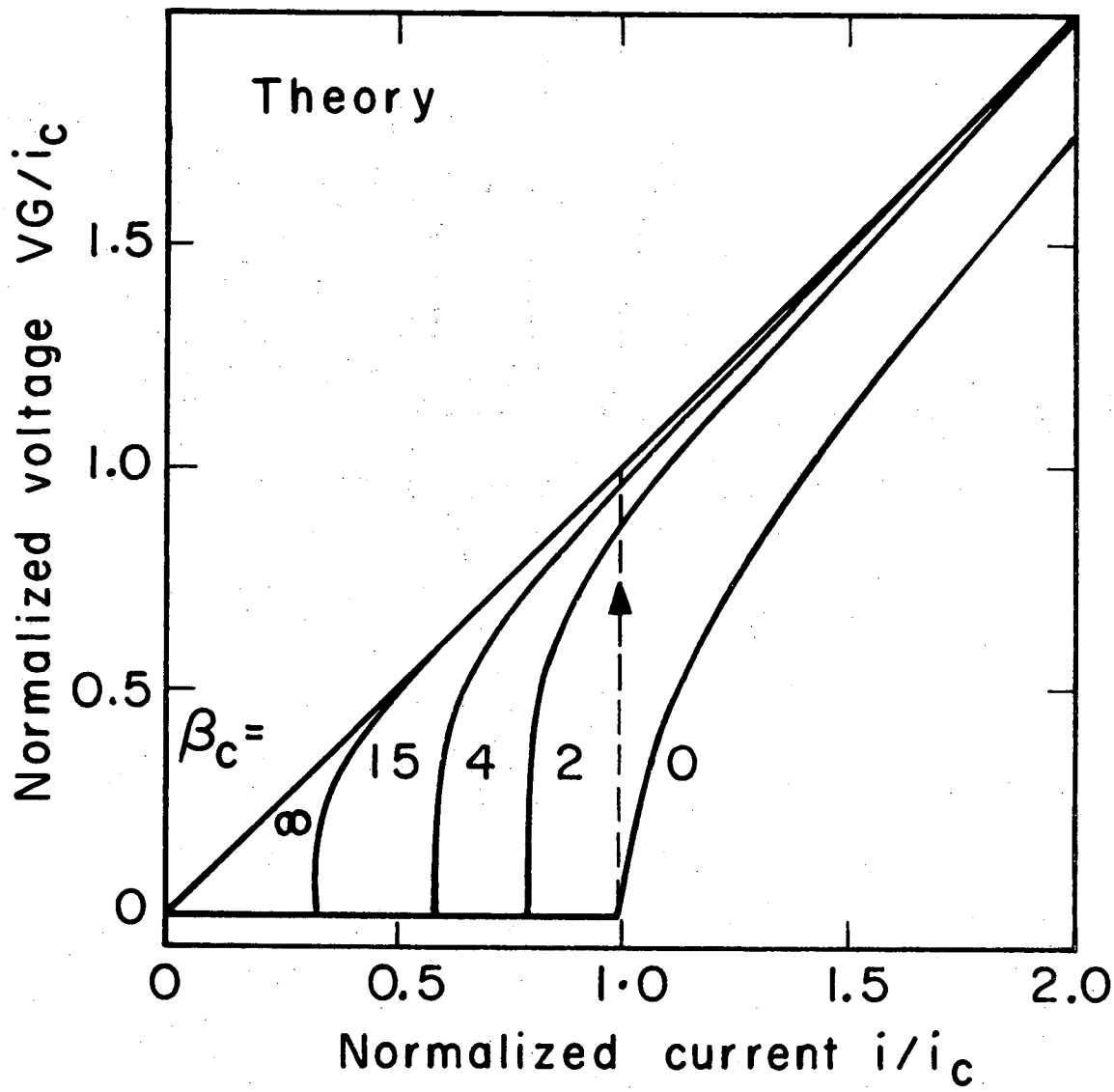

XBL715-3604

Fig. 3

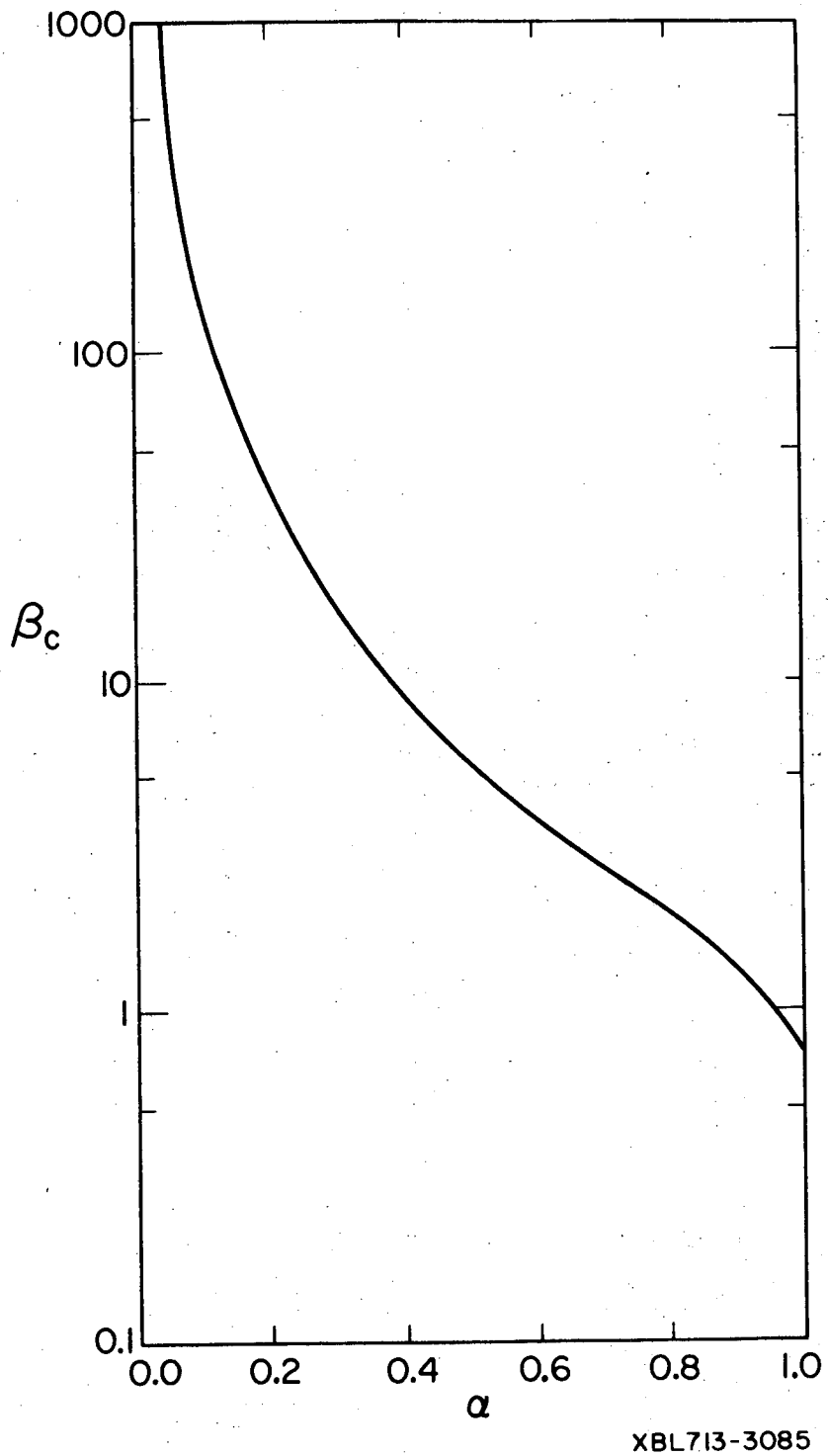

Fig. 4

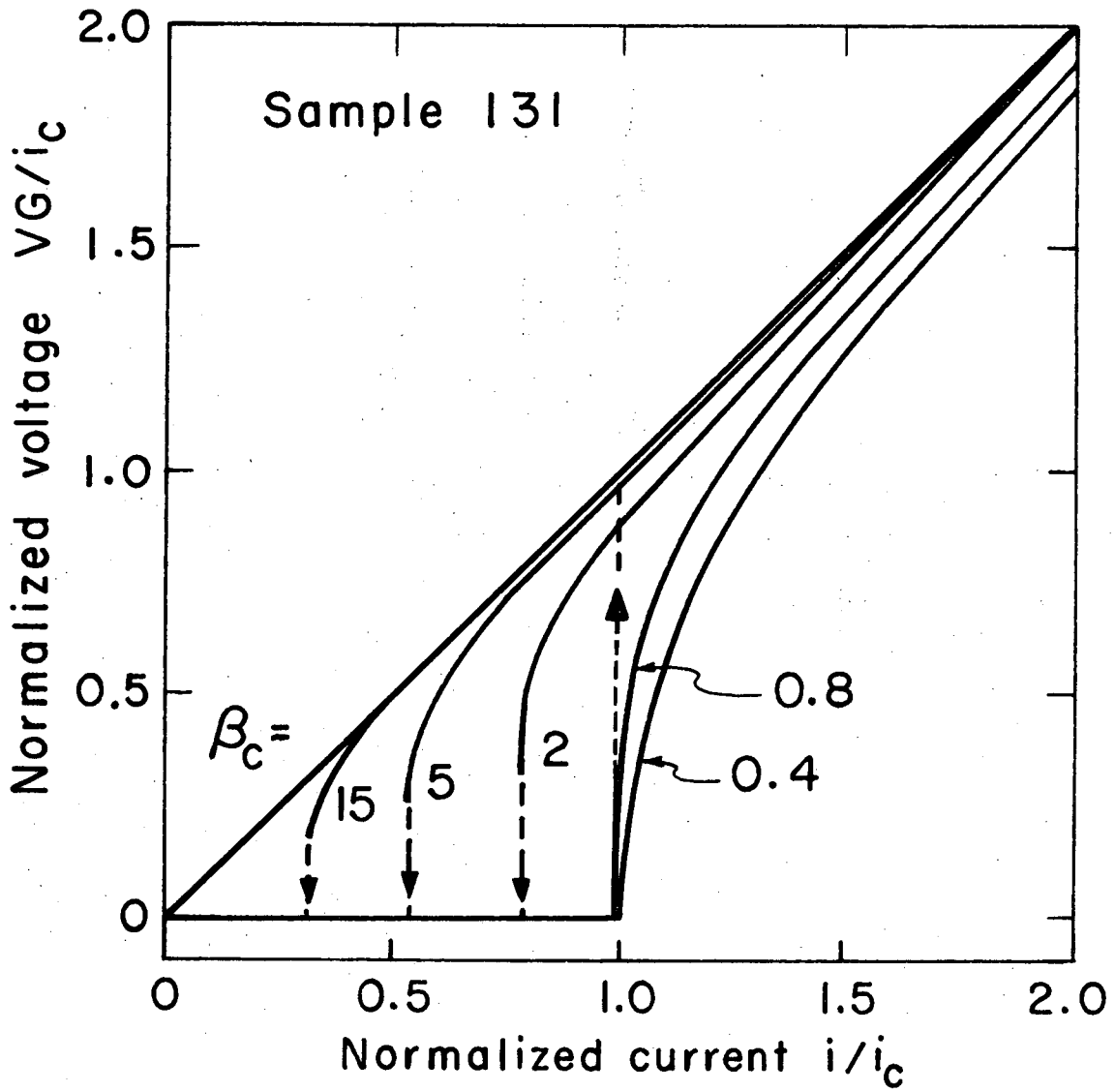

XBL715-3605

Fig. 5

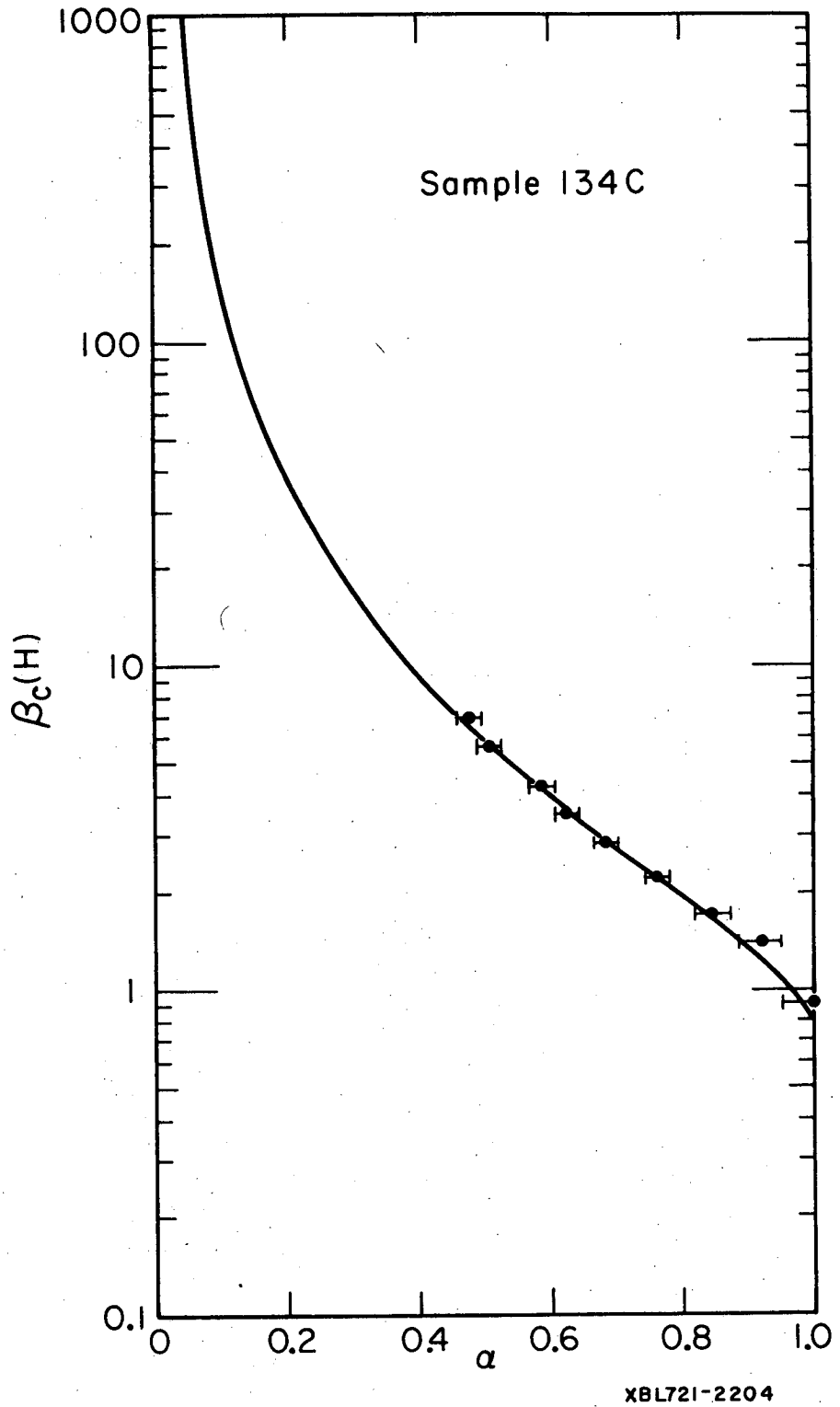
1000
100
10
1
0.1
$\beta_c(H)$
Sample 134C
0
0.2
0.4
0.6
0.8
1.0
α
XBL721-2204

Fig. 6

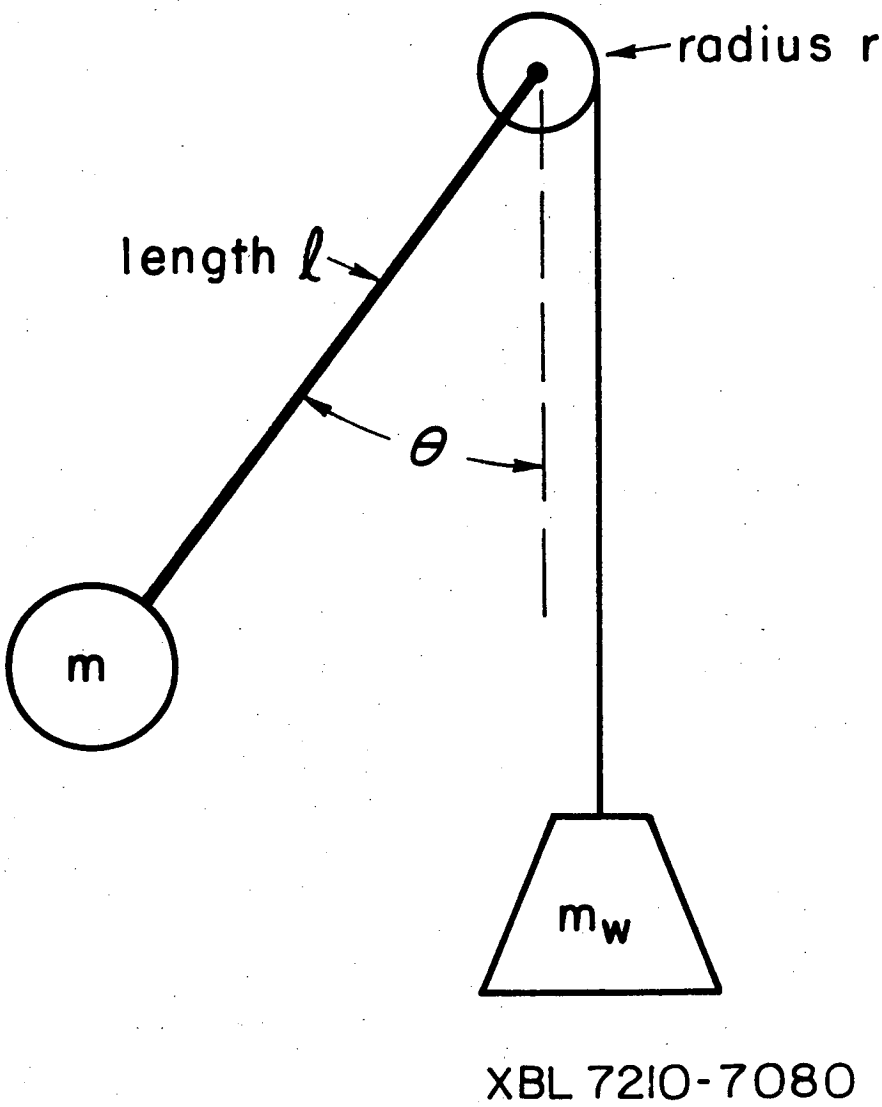

Fig. 7

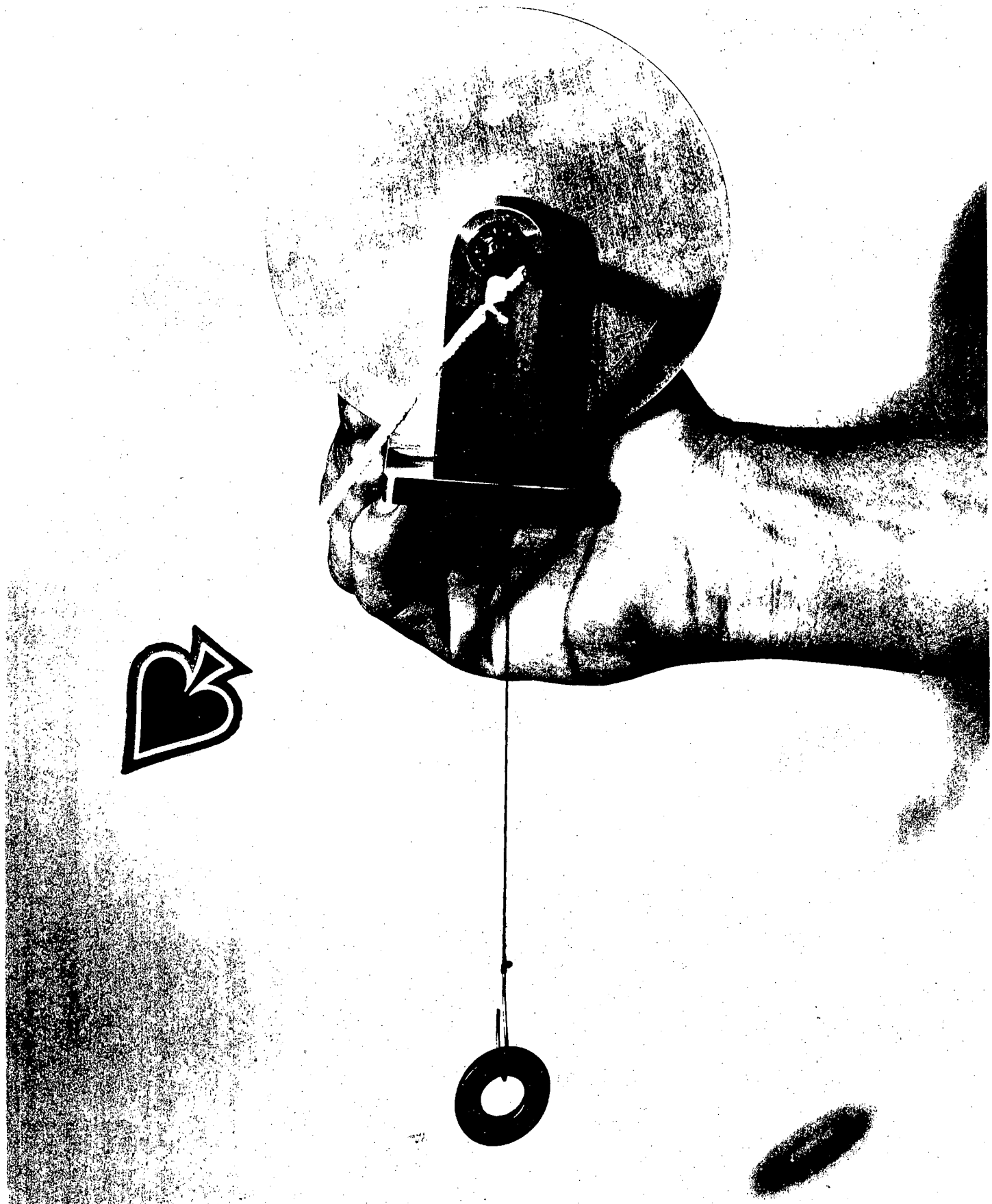

Fig. 8a

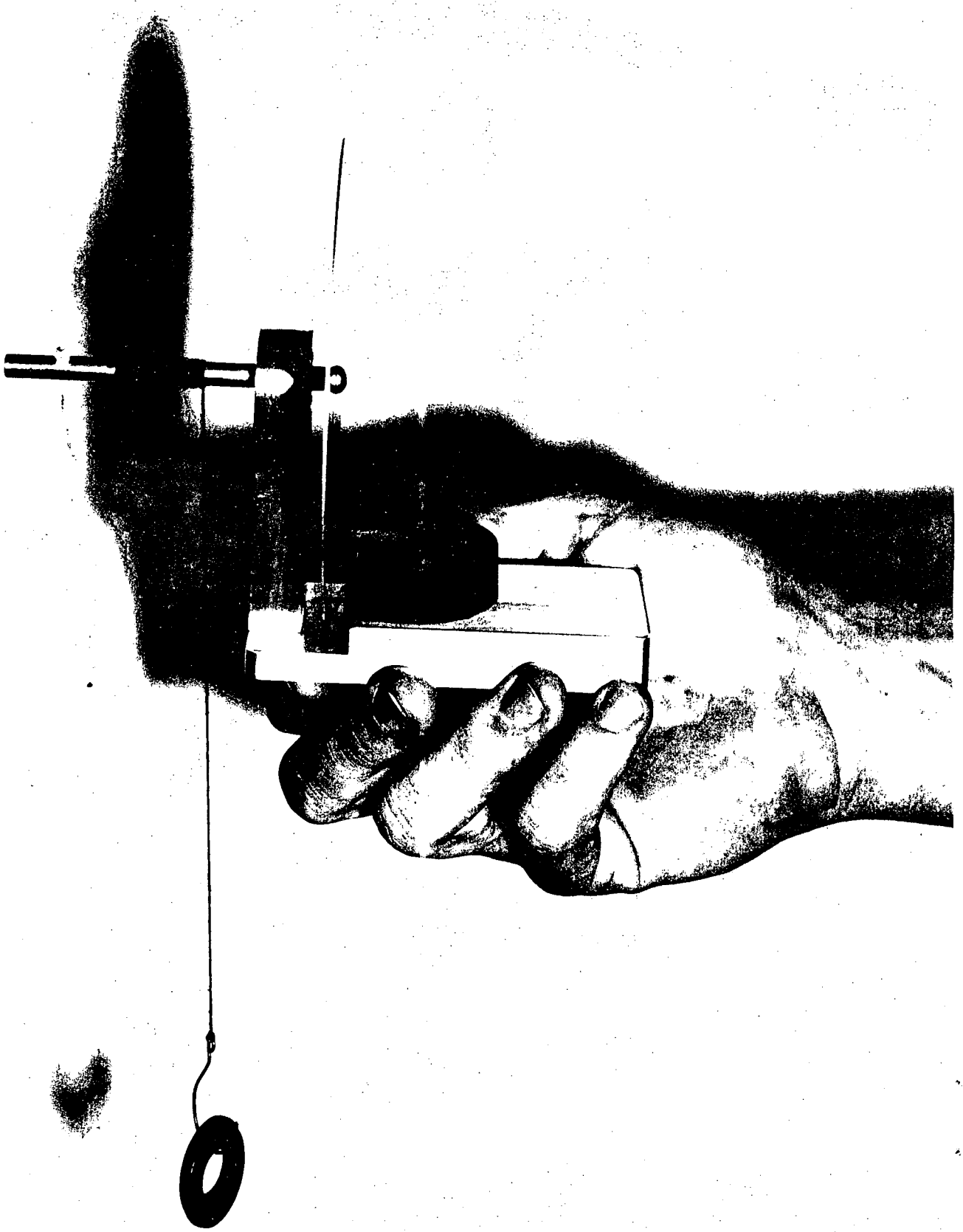

Fig. 8b

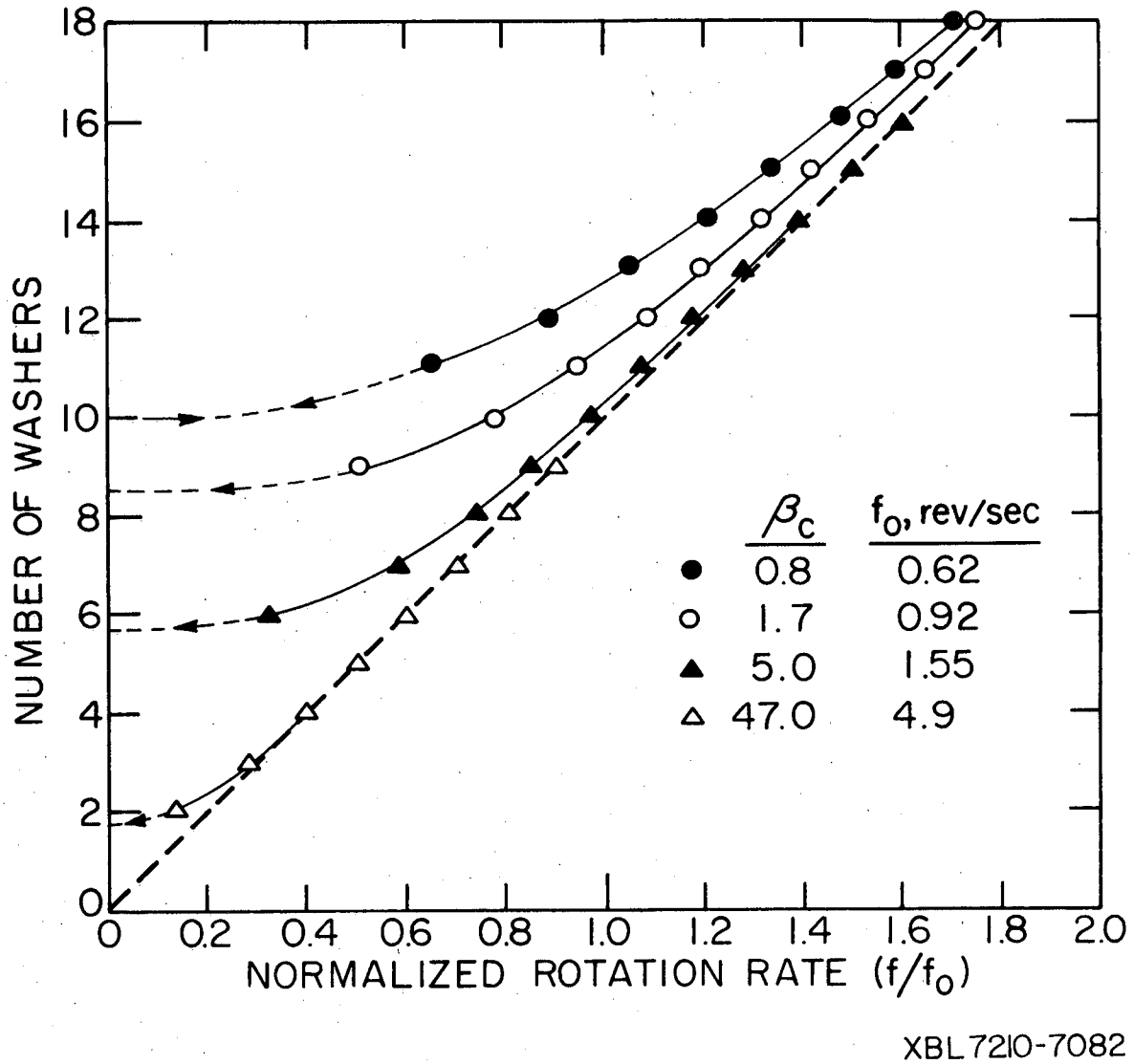

XBL7210-7082

Fig. 9

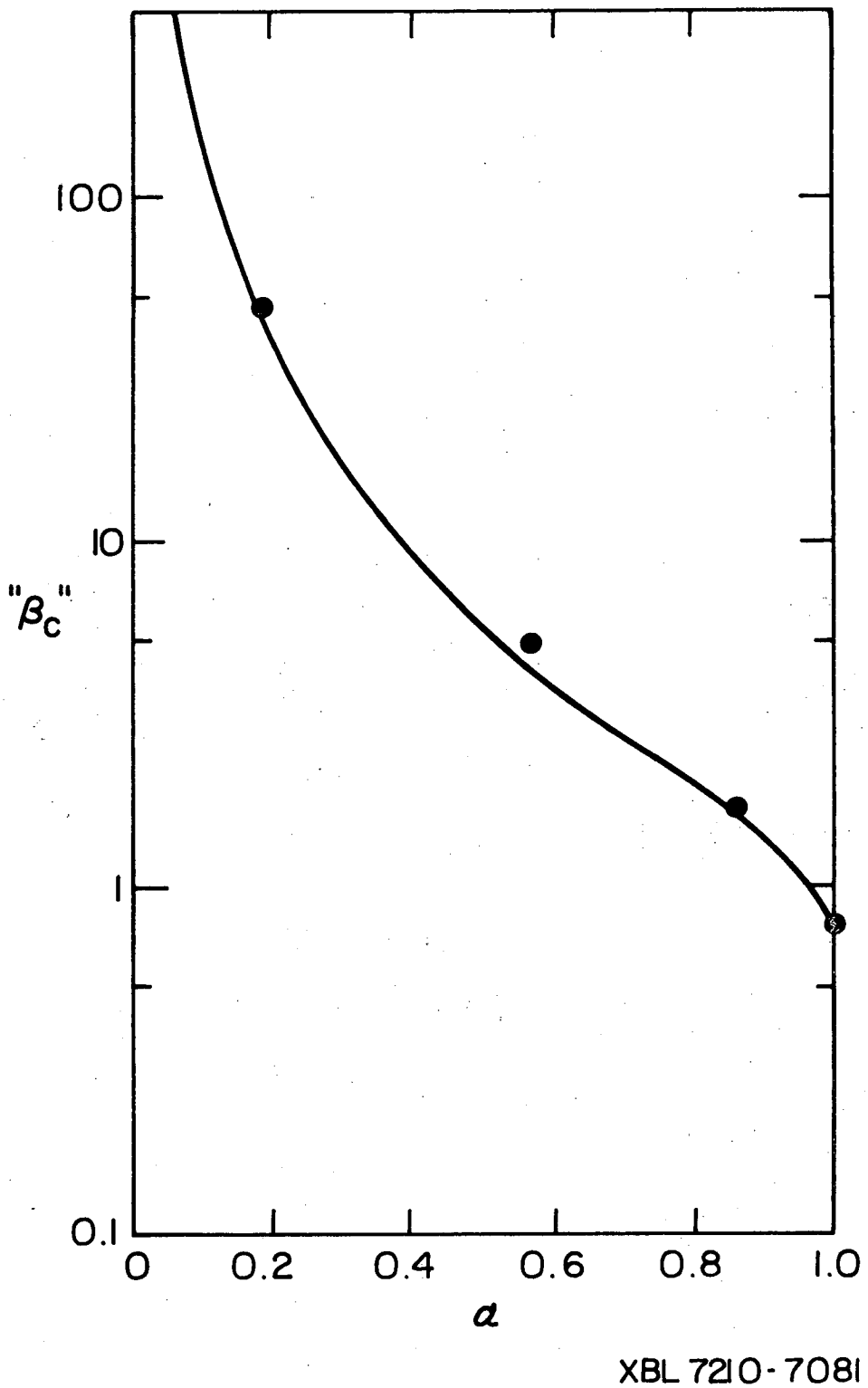

Fig. 10

TECHNICAL INFORMATION DIVISION
LAWRENCE BERKELEY LABORATORY
UNIVERSITY OF CALIFORNIA
BERKELEY, CALIFORNIA 94720